

Numerical Solution for Magnetohydrodynamics Mixed Convection Flow Near a Vertical Porous Plate Under the Influence of Magnetic Effect and Velocity Ratio

Ibrahim Yusuf¹, Umaru Mohammed¹ and Khadeejah James Audu¹

¹Department of Mathematics, Federal University of Technology, Minna, Niger state, Nigeria.

E-mail: ibrahimy338@gmail.com

Abstract

This paper investigates the effects of thermal radiation on MHD mixed convection flow, heat and mass transfer, Dufour and Soret effects over a porous plate having convective boundary condition under the influence of magnetic field. The governing boundary layer equations are formulated and transformed into nonlinear ordinary differential equations using similarity transformation and numerical solution is obtained by using Runge-Kutta fourth order scheme with shooting technique. The effects of various physical parameters such as velocity ratio parameter, mixed convection parameter, melting parameter, suction parameter, injection parameters, Biot number, magnetic parameter, Schmit and prandtl numbers on velocity and temperature distributions are presented through graphs and discussed.

Keywords: Dufour effect, Magnetohydrodynamics, Mixed convection, Melting, Soret effect.

1. Introduction

Magnetohydrodynamics (MHD), also called magneto-fluid dynamics or hydromagnetics is a model of electrically conducting fluids that treats all interpenetrating particle species together as a single continuous medium. It is primarily concerned with the low-frequency large-scale, magnetic behavior in plasmas and liquid metals and has applications in numerous fields including geophysics, astrophysics, engineering and medical sciences Saman *et al.* (2017). The field of MHD was initiated by Hannes Alfven 1942 for which he received noble prize in physics in 1970. The fundamental concept behind MHD is that magnetic field can induce currents in a moving conductive fluid, which in turn creates forces on the fluid and changes the magnetic field itself. The set of equations that describe MHD are combination of the Navier-Stokes equations of fluid dynamics and Maxwell's equation of electromagnetism. The effects of mass transfer on MHD second grade fluid towards stretching cylinder was explored by Alamri *et al.* (2019) analytically using homotopy analysis method and reported that the velocity decreases with increasing values of magnetic field.

Mixed convection occurs when heat transfer in a fluid or gas is influenced by both forced convection and natural convection. Forced convection is induced by external factors like fans or pumps, while natural convection occurs due to temperature gradients causing density differences. When both forced and natural convection effects are comparable, it is referred to as mixed convection Davood and Sayyid (2015). This phenomenon is important in scenarios where both mechanisms play a significant role, such as in complex ventilation systems, heat exchangers, and electronic cooling systems. Understanding the characteristics and mechanisms of mixed convection is crucial for improving heat transfer and designing efficient thermal management systems (Aaiza *et al.* 2015).

Dufour and Soret are two important mass transfer mechanism in fluid dynamics and heat transfer. The Dufour and Soret effects are two related phenomena that occur in multi-component systems, particularly in the field of fluid dynamics. These effects are named after two Swiss physicists, Jean-Baptiste Dufour and Charles Soret, who made significant contributions to understanding the behavior of mixtures and diffusion in the 19th century (Venkata *et al.* 2021).

2. Literature review

Jha and Mohammed (2014) studied mixed convection effect on melting from a vertical plate embedded in porous medium with Soret and Dufour effects. Jha *et al.* (2013) studied the effects of Dufour and Soret on melting from a vertical plate embedded in saturated porous medium. Sharma *et al.* (2018) studied the influence of heat source on MHD mixed convection stagnation point flow along a vertical stretching sheet. Reddy and Ali (2016) investigated the combined influence of suction and thermophoresis on the mixed convective mass transfer boundary layer flow of micropolar fluids through porous medium over a stretching sheet in the presence of thermo-Diffusion and Diffusion-thermo effects. Jha and Muhammad (2019) investigated the chemical reaction and diffusion thermo effect on steady fully developed free convection heat and mass transfer flow near an infinite vertical moving porous plate under nonlinear Boussinesq approximations. The impact of nonlinear thermal radiation on nonlinear mixed convection flow near a vertical porous plate with convective boundary condition has been investigated by Jha and Samaila (2020; 2021a; 2021b; 2022). Surbhi *et al.* (2023) studied the numerical investigation of micropolar fluid flow due to melting stretchy surface in a porous medium. Hemalatha and Prasad (2014) investigated the analysis of melting phenomenon with mixed convection flow and heat transfer in a fluid saturated porous medium considering the effect of applied magnetic field, viscous dissipation, and radiation by taking forchheimer extension.

Motivated by the aforementioned papers, the combined effects of magnetic effect and velocity ratio on MHD mixed convection flow has not been studied. Hence, this paper is aimed at establishing a mathematical model to analyze the effect of magnetic effect and velocity ratio on MHD mixed convection flow near a vertical porous plate with thermal radiation.

3. Methodology

Consider a hydrodynamic and boundary layer flow on a vertical porous plate influence by nonlinear thermal radiation as shown in figure 3.1. As demonstrated in the figure, the fluid is assume to move with a uniform velocity U_∞ far away from the vertical porous plate at a temperature T_∞ , whereas the porous plate surface is heated through convection from a hot fluid at a temperature T_f with a heat transfer coefficient h_f . Here, the momentum equation is subjected to the Boussinesq approximation.

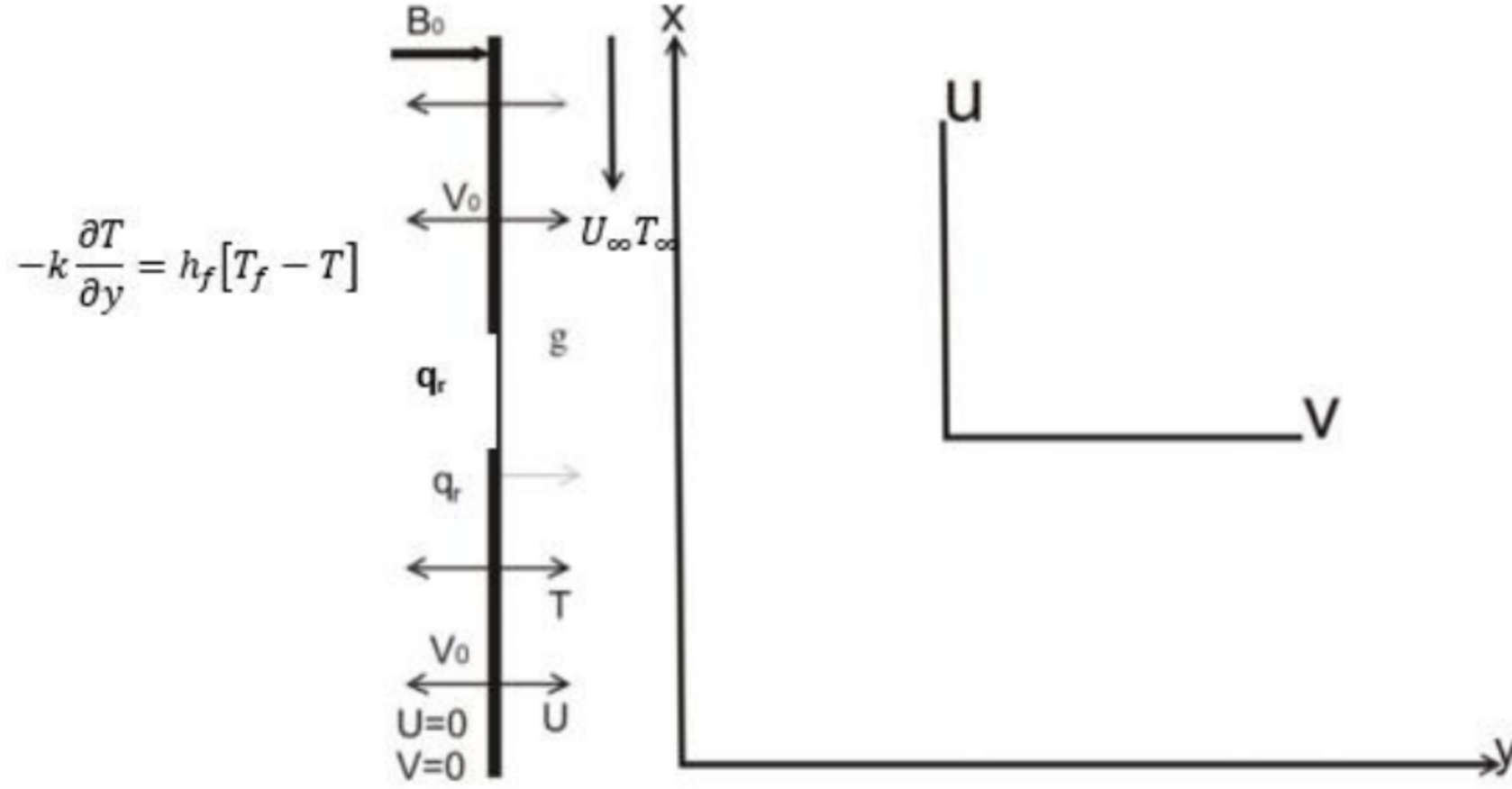


Figure 3.1: Flow configuration

Following (Jha and Samaila 2021a), the equation that governs the flow of fluid is defined as:

$$\frac{\partial u}{\partial x} + \frac{\partial v}{\partial y} = 0, \quad (1)$$

$$u \frac{\partial u}{\partial x} + v \frac{\partial u}{\partial y} = \nu \frac{\partial^2 u}{\partial y^2} - \frac{\sigma B_0^2}{\rho_f} (u - u_\infty) + g\beta(T - T_\infty), \quad (2)$$

$$u \frac{\partial T}{\partial x} + v \frac{\partial T}{\partial y} = \alpha \left[\frac{\partial^2 T}{\partial y^2} - \frac{1}{K} \frac{\partial q_r}{\partial y} \right] \quad (3)$$

Where T denote the dimensional temperature, K denote thermal conductivity, U denote velocity, ν denote kinematic viscosity, and (u, v) are the velocity components. The quantity q_r is the radiative heat flux. However, the radiative heat flux in the x -direction is assumed to be small in comparison to that in y -direction. According to Jha *et al.* (2018), the radioactive heat flux q_r can be simplified through Rosseland diffusion approximation for an optical thick fluid as

$$q_r = -\frac{4\sigma\partial T^4}{3k^*\partial y} \quad (4)$$

Where σ and K^* represent the Stefan Boltzman constant and mean absorption respectively. Though, Rosseland approximation is only applicable for an optical thick fluid. Regardless of these limitations, it has been applied in several investigations particularly from the analysis of radiation effect on blast waves by the nuclear explosion to the transport of radiation through gasses at low density (Agha *et al.* 2014).

The boundary conditions related to the present analysis can be written as:

$$\left. \begin{aligned} u(x, y = 0) = 0, v(x, y = 0) = \frac{c}{a}, -k \frac{\partial T}{\partial y}(x, y = 0) &= h_f [T_f - T(x, y = 0)] \\ u(x, y \rightarrow \infty) = U_\infty, T(x, y \rightarrow \infty) &= T_\infty, \end{aligned} \right\} \quad (5)$$

The following similarity transformations are introduced to transform equation (2) and (3).

$$\left. \begin{aligned} \eta &= y \sqrt{\frac{U_\infty}{\nu x}}, \\ u &= U_\infty f'(\eta) \\ v &= \frac{1}{2} \sqrt{\frac{U_\infty \nu}{x}} (\eta f'(\eta) - f), \\ \theta &= \frac{T - T_\infty}{T_f - T_\infty} \end{aligned} \right\} \quad (6)$$

Substituting equation (4) – (6) in equation (2) and (3), the momentum and energy equations and the boundary conditions are reduced to;

$$f''(\eta) + \frac{1}{2} f(\eta) f''(\eta) + M(1 - f') + Gr_x \theta(\eta) = 0 \quad (7)$$

$$\theta''(\eta) \left(1 + \frac{4}{3} R(\theta + C_T)^3 \right) + 4R((C_T + \theta)^2 (\theta'(\eta))^2) + \frac{1}{2} Pr \theta'(\eta) f(\eta) = 0 \quad (8)$$

The appropriate boundary conditions are

$$\left. \begin{aligned} f(0) &= S, \\ f'(0) &= A, \\ \theta'(0) &= -Bi[1 - \theta(0)] \\ f'(\infty) &= 1, \\ \theta(\infty) &= 0, \end{aligned} \right\} \quad (9)$$

Where prime denotes derivative with respect to η , $Gr_x = \frac{\nu x g \beta (T_f - T_\infty)}{U_\infty^2}$ is local Grashof number, $Pr = \frac{\mu c_p}{K}$ is the prandtl number, $Bi = \frac{h_f}{k} \sqrt{\frac{\nu x}{U_\infty}}$ is local convective heat transfer parameter, $S = \frac{-2\nu_0}{\sqrt{U_\infty \nu}}$ is suction/injection parameter, $R = \frac{4\sigma(T_f - T_\infty)^3}{k^* k}$ non linear thermal radiation parameter, $C_T = \frac{T_\infty}{T_f - T_\infty}$ temperature difference, $M = \frac{\sigma x \beta_0^2}{\rho_f}$ magnetic term parameter, $A = \frac{c}{a}$ is velocity ratio parameter.

4. Results and Discussion

The analysis of the effect of melting, Dufour and Soret effect on MHD mixed convection flow near a vertical porous plate with thermal radiation is presented. The effect of the convective boundary conditions at the porous plate surface is considered. The governing equations were transformed using similarity transformation and are solved through Maple using the RKF45 algorithm. RKF45 is a default numeric scheme in Maple software because of its accuracy and robustness. To ascertain the accuracy of the present analysis, comparisons have been made with previous literature which shows good correlation. The implication of parameters affecting fluid transport is analyzed. The default values of these flow factors are regarded as $S = 1.0$, $M = 1.5$, $Gr_x = 0.5$, $A = 0.5$, $B = 0.1$, $R = 1.0$, $Pr = 0.72$, $U = C_T = S_c = 0.4$, $Kr = 0.2$, $Me = 0.2$ and $Df(Sr) = 0.03(2.0)$.

Table 4.1: Comparison of the present results to the work of Jha and Samaila in the absence of suction/injection, magnetic effect and velocity ratio.

				Jha and Samaila (2021a)			Present Work		
Bi_x	Gr_x	Pr	R	$f''(0)$	$-\theta'(0)$	$\theta(0)$	$f''(0)$	$-\theta'(0)$	$\theta(0)$
0.1	0.1	0.72	0.1	0.36911	0.07493	0.25069	0.36911	0.07493	0.25069
1.0	0.1	0.72	0.1	0.44445	0.22287	0.77713	0.44445	0.22287	0.77713
10	0.1	0.72	0.1	0.47273	0.26702	0.97330	0.47273	0.26702	0.97330
0.1	0.5	0.72	0.1	0.49816	0.07601	0.23987	0.49816	0.07601	0.23987
0.1	1.0	0.72	0.1	0.63384	0.07693	0.23066	0.63384	0.07693	0.23066
0.1	0.1	2.0	0.1	0.35380	0.08096	0.19036	0.35380	0.08096	0.19036
0.1	0.1	7.0	0.1	0.34283	0.08663	0.13366	0.34283	0.08663	0.13366
0.1	0.1	0.72	0.5	0.37033	0.07433	0.25669	0.37033	0.07433	0.25669
0.1	0.1	0.72	0.1	0.37195	0.07354	0.26452	0.37195	0.07354	0.26452

The accuracy of the current code is illustrated in Tables 4.1, where the comparison is performed without considering suction/injection, magnetic effect, and velocity ratio parameters. The table showcases the utilization of nonlinear ODEs, employing constant values of Bi_x , Gr_x , Pr , and R while setting the suction/injection, magnetic effect, and velocity ratio values to zero. The results obtained from the present work align with the findings of Jha and Samaila (2021a).

Table 4.2: Comparison of the present approach with Jha and Samaila (2021a) on the Nusselt number $-\theta(0)$ for $Gr_x = S = R = A = M = 0$

Jha and Samaila (2021a)				Present work		
Bi_x	$Pr = 0.1$	$Pr = 0.72$	$Pr = 0.10$	$Pr = 0.1$	$Pr = 0.72$	$Pr = 0.10$
0.05	0.036844	0.042767	0.046787	0.036844	0.042767	0.046787
0.10	0.058338	0.074724	0.087925	0.058338	0.074724	0.087925
0.20	0.082363	0.119295	0.156903	0.082363	0.119295	0.156903
0.40	0.103720	0.169994	0.258174	0.103720	0.169994	0.258174
0.60	0.113533	0.198051	0.328945	0.113533	0.198051	0.328945
0.80	0.119170	0.215864	0.381191	0.119170	0.215864	0.381191
1.0	0.122830	0.228178	0.421344	0.122830	0.228178	0.421344
5.0	0.136215	0.279131	0.635583	0.136215	0.279131	0.635583
10	0.138096	0.287146	0.678721	0.138096	0.287146	0.678721
20	0.139056	0.291329	0.702563	0.139056	0.291329	0.702563

Table 4.2 examines the non-linear ODEs for model equations without considering the effects of nonlinear thermal radiation, suction/injection, and magnetic effect. It focuses on the scenario where Bi_x tends to infinity. The table illustrates the influence of Bi_x on the Nusselt number $-\theta'(0)$, revealing that as the values of Bi_x increase, the Nusselt number appreciates for $Pr = 0.1$, $Pr = 0.72$, and $Pr = 0.10$. This finding supports the results obtained by Jha and Samaila (2021a).

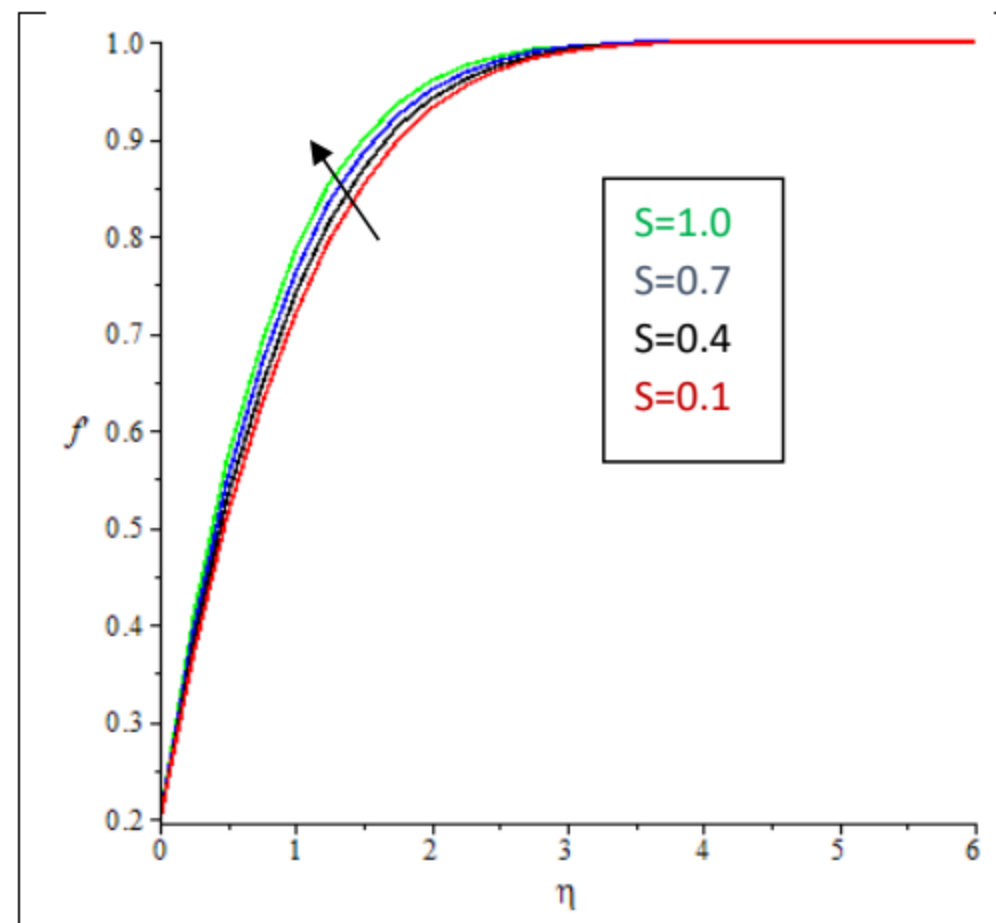


Figure 4.1: Effect of $S > 0$ Variations on $f'(\eta)$

The effect of suction on the fluid velocity distribution is depicted in figure 4.1, it is observed from the figure that the velocity f' increase as the suction $S > 0$ increases. This is because when suction increases the velocity profile is altered. The increase in suction parameter result in an increase in the velocity of the fluid near the surface where the suction is applied, this leads to narrowing of the boundary layer near the surface as the higher velocity at the surface causes greater amount of shear stress which in turn reduces the thickness of the boundary layer.

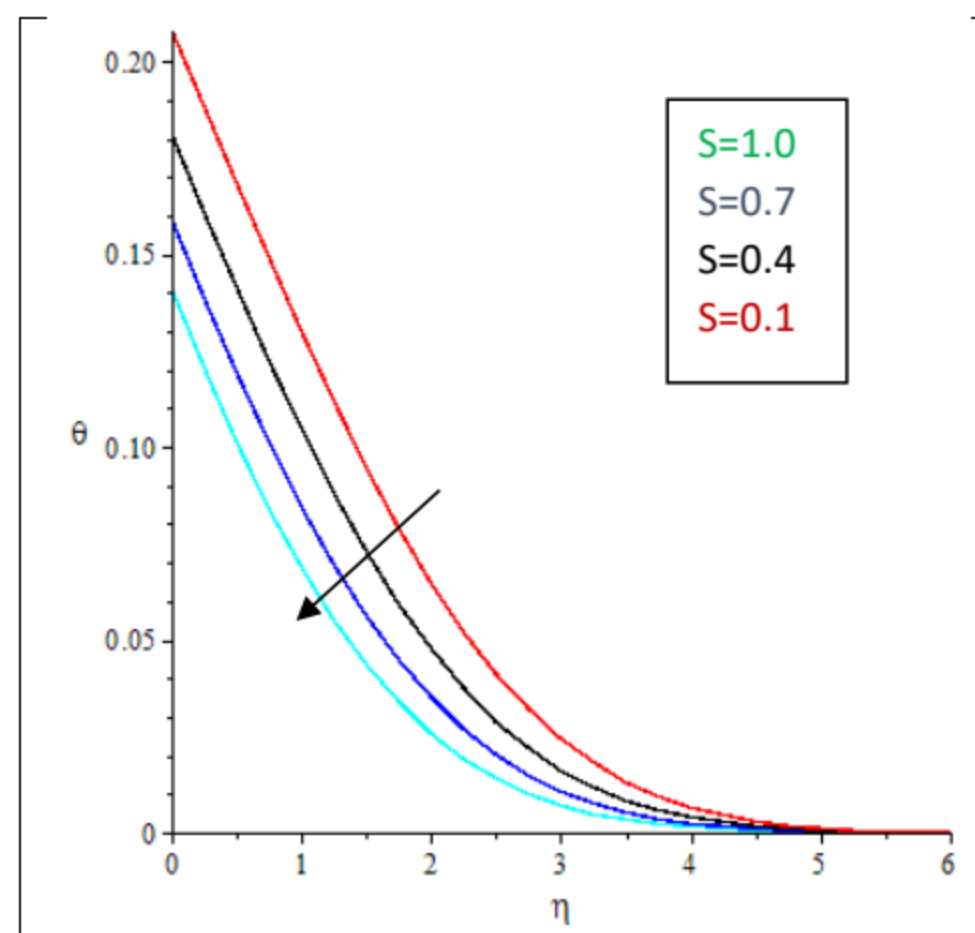


Figure 4.2: Effect of $S > 0$ Variations on $\theta(\eta)$

Figure 4.2 depict the effect of suction $S > 0$ on temperature. As shown from the figure, the temperature distribution is decrease due to the increase in suction. This is because when there is an increase in suction $S > 0$, there is more pressure being exerted on the fluid. This increase pressure can cause the fluid to flow more quickly which in turn leads to decrease in temperature of the fluid. Because, as the fluid flows more quickly it can exchange heat with its surrounding more easily. This result in a cooling effect on the fluid leading to a decrease in temperature and a thinner boundary layer.

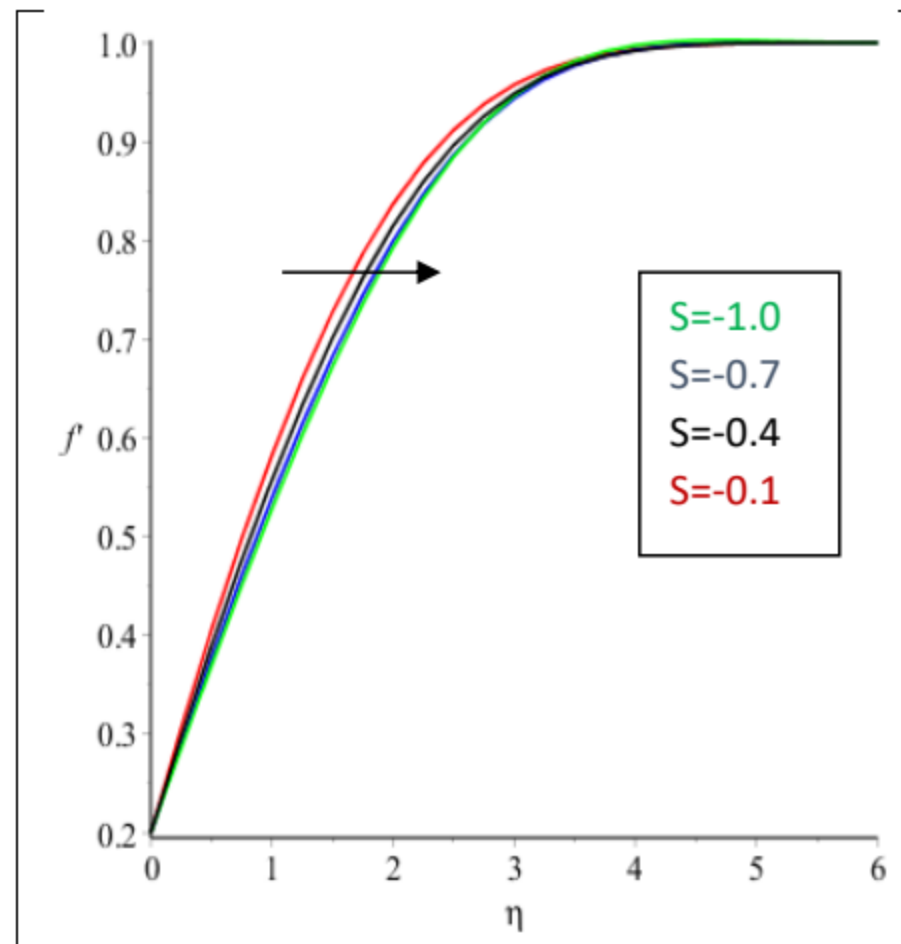


Figure 4.3: Effect of $S < 0$ Variations on $f'(\eta)$

Figure 4.3 shows the effect of injection $S < 0$ on velocity profile. As depicted from the figure the fluid velocity decreases as η increases. This indicates that with injection growth the velocity profile of the system decreases. That is, as injection parameter increases the velocity profile decreases. Because increasing the injection parameter causes more fluid to be injected into the system, increasing the overall volume and the flow rate of the fluid. This can lead to a higher pressure drop and increased turbulence within the system, resulting in a decrease in the velocity profile and a thicker boundary layer.

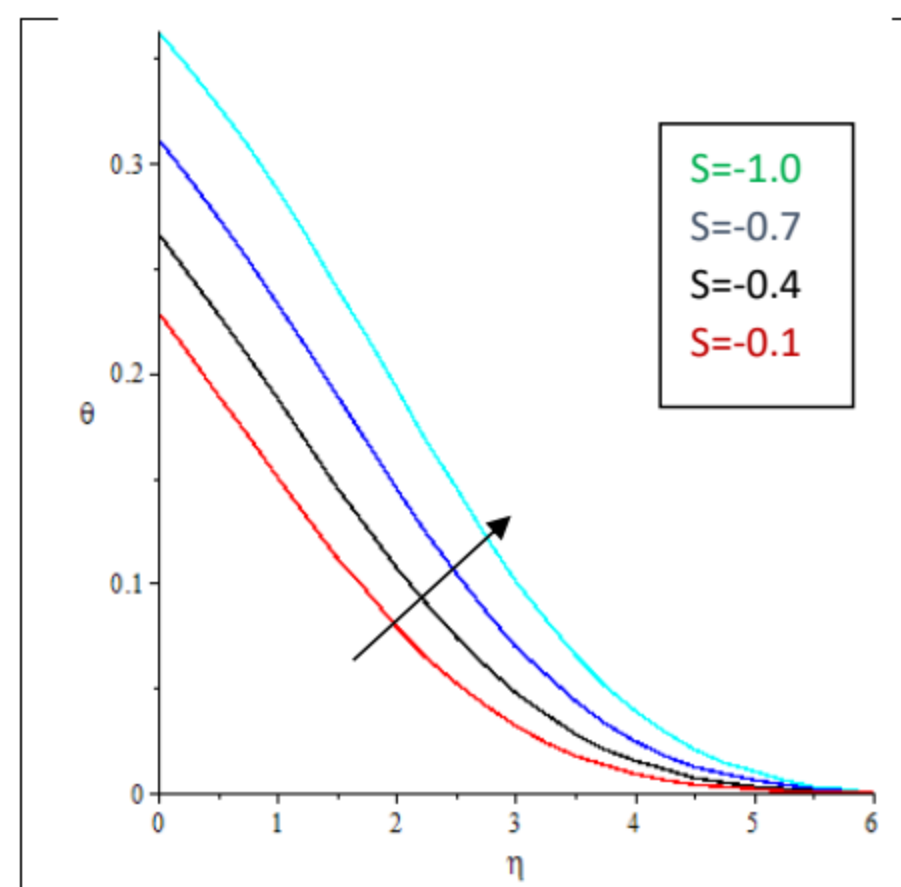


Figure 4.4: Effect of $S < 0$ Variations on $\theta(\eta)$

Figure 4.4 show the effect of injection parameter variation on temperature. As illustrated from the figure, the fluid temperature increases as η increases. This indicates that as injection parameter increases there is a corresponding increase in the temperature of the fluid. Hence, an increase in injection parameter enhances the

temperature profile of the fluid. the reason for the increase in the temperature profile is because when injection increases, there is a higher amount of energy being introduced into the fluid. This can be in the form of flow rate, pressure, or a combination of both. As a result, the fluid is being subjected to more turbulent mixing and increase friction within the system leading to an increase in temperature.

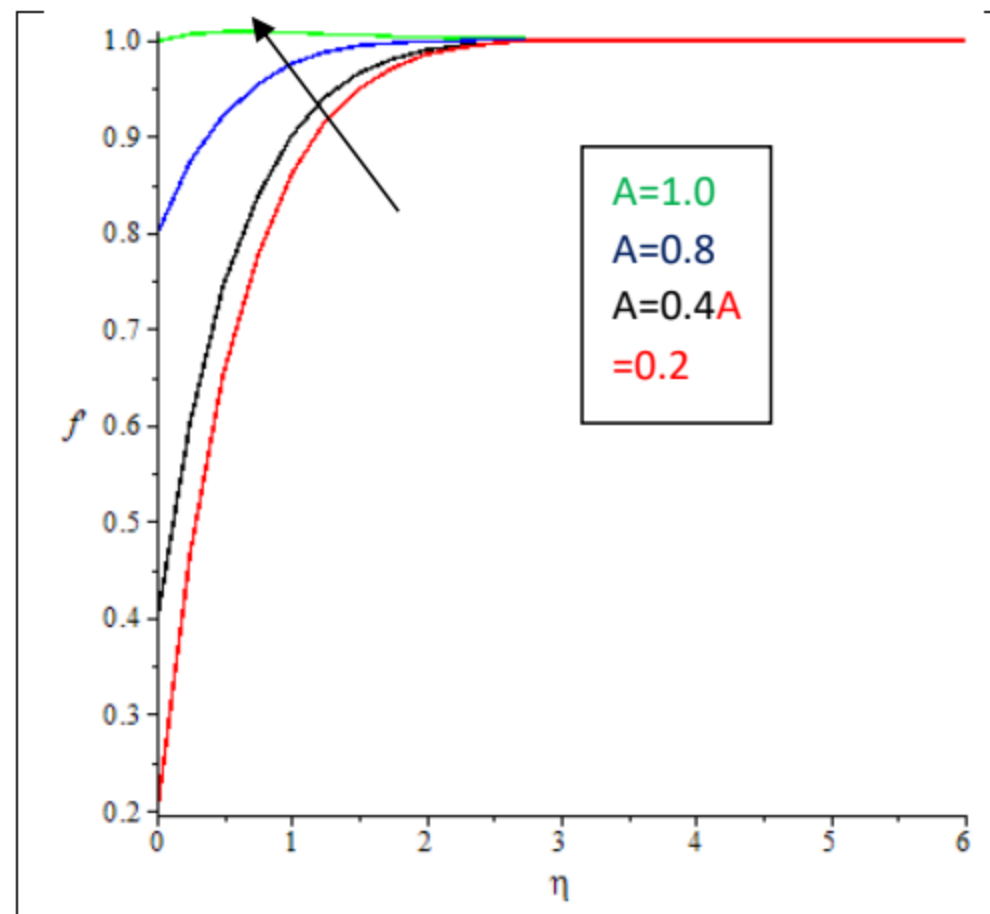


Figure 4.5: Effect of Velocity Ratio parameter A Variation on $f'(\eta)$

Figure 4.5 depict the resultant effect of velocity ratio parameter A variation on velocity profile $f'(\eta)$, which shows that as velocity ratio parameter A increases, the fluid velocity increases for both assisting and opposing flow. This is because the stretching velocity dominates the free stream velocity.

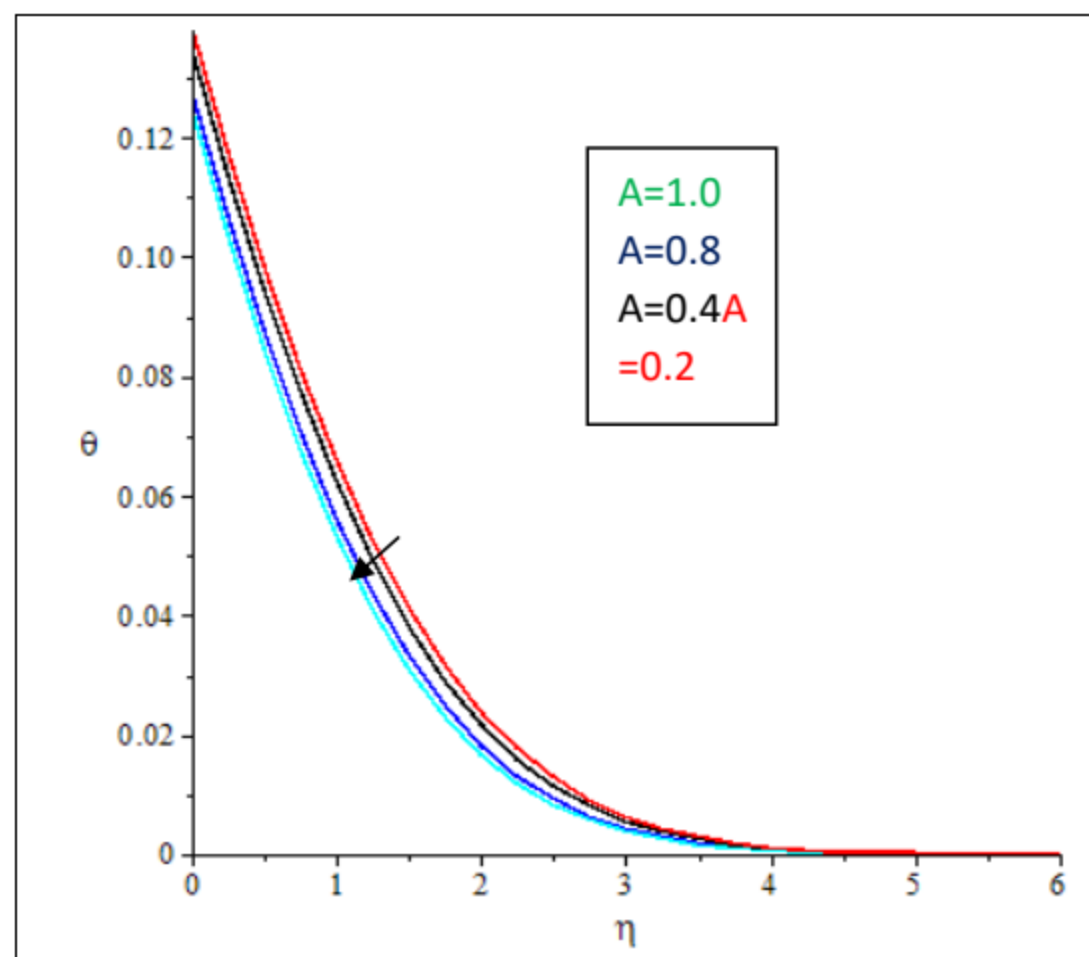


Figure 4.6: Effect of Velocity Ratio Variations on $\theta(\eta)$

Figure 4.6 depict the effect of velocity ratio parameter A variation on temperature profile. As illustrated from the figure, as velocity ratio parameter A increases the temperature profile decreases. This is because as velocity ratio parameter A increases the velocity of the system increases more rapidly, due to this the temperature profile decreases.

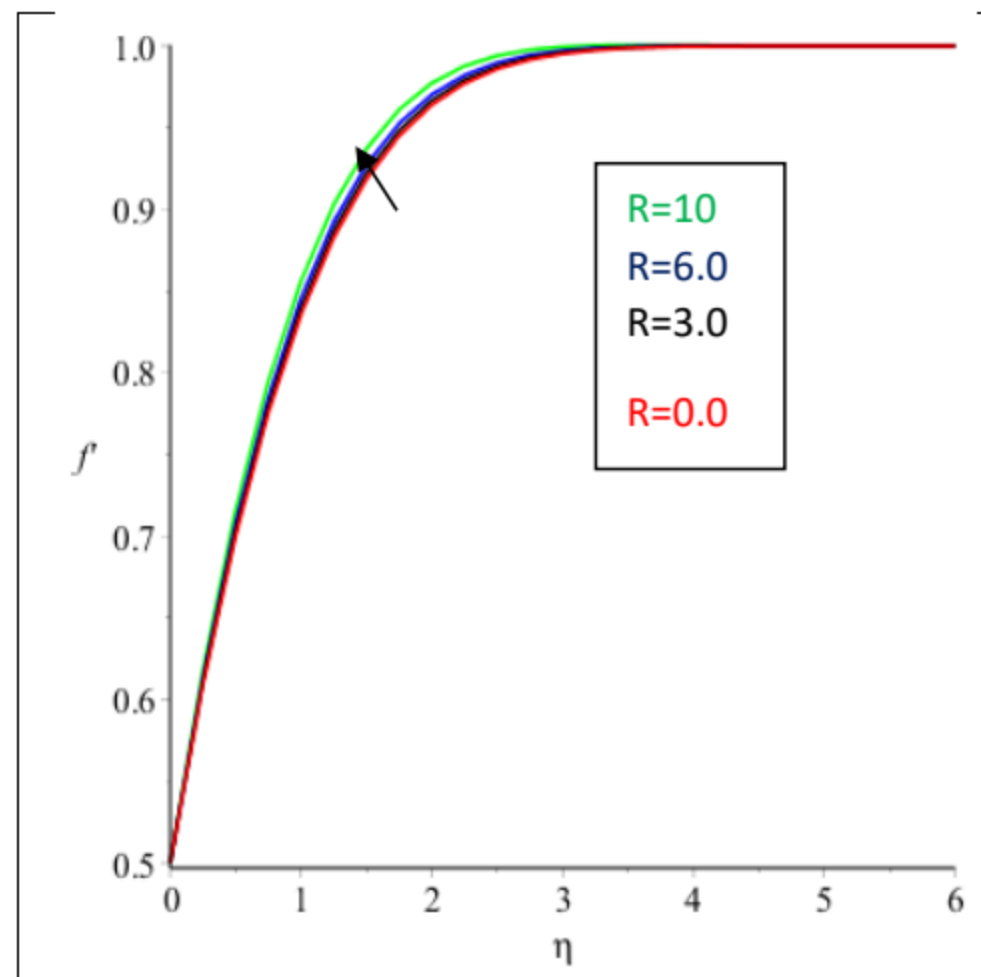


Figure 4.7: Effect of Radiation Parameter Variations on $f'(\eta)$

Figure 4.7 depict the resultant effect of Radiation Parameter R variation on velocity profile $f'(\eta)$, which shows that as Radiation Parameter R increases, the fluid velocity also increases. Hence, an increase in Radiation Parameter R enhanced the velocity profile of the fluid. This is because radiation heat transfer can contribute to the energy balance of the fluid. When radiation heat transfer is increased, more heat is transferred to the fluid, causing it to become warmer and less dense. As a result, the fluid becomes more buoyant and rises at a faster rate, leading to an increase in fluid velocity.

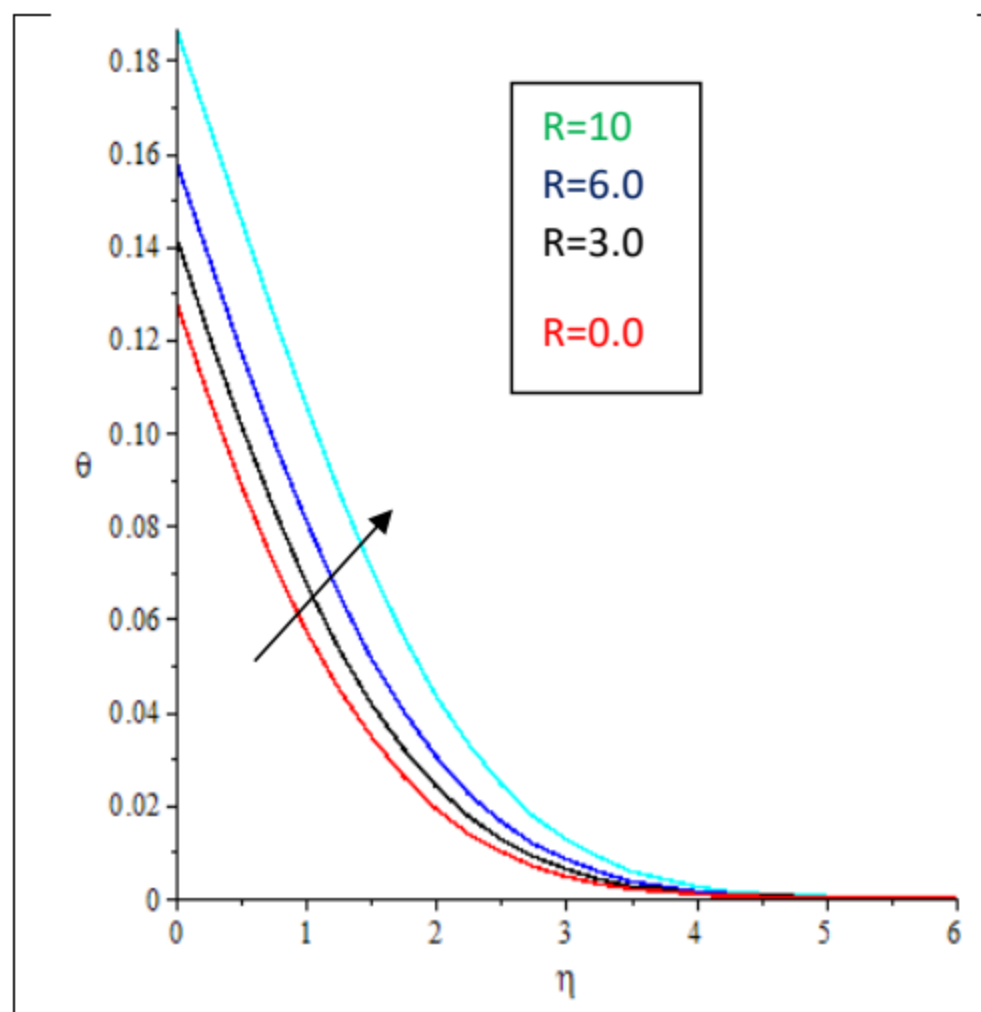


Figure 4.8: Effect of Radiation Parameter R Variations on $\theta(\eta)$

Figure 4.8 depict the resultant effect of Radiation Parameter R variation on temperature profile, which shows that as Radiation Parameter R increases, there is a corresponding increase in the temperature of the fluid. Hence, as the Radiation Parameter R increases the temperature profile of the fluid is enhanced. This is because radiation

helps in transferring heat energy from one medium to another without the need of contact. This means that as radiation parameter increases, more heat energy is being transferred to the fluid causing it to heat up and leading to an increase in its temperature profile.

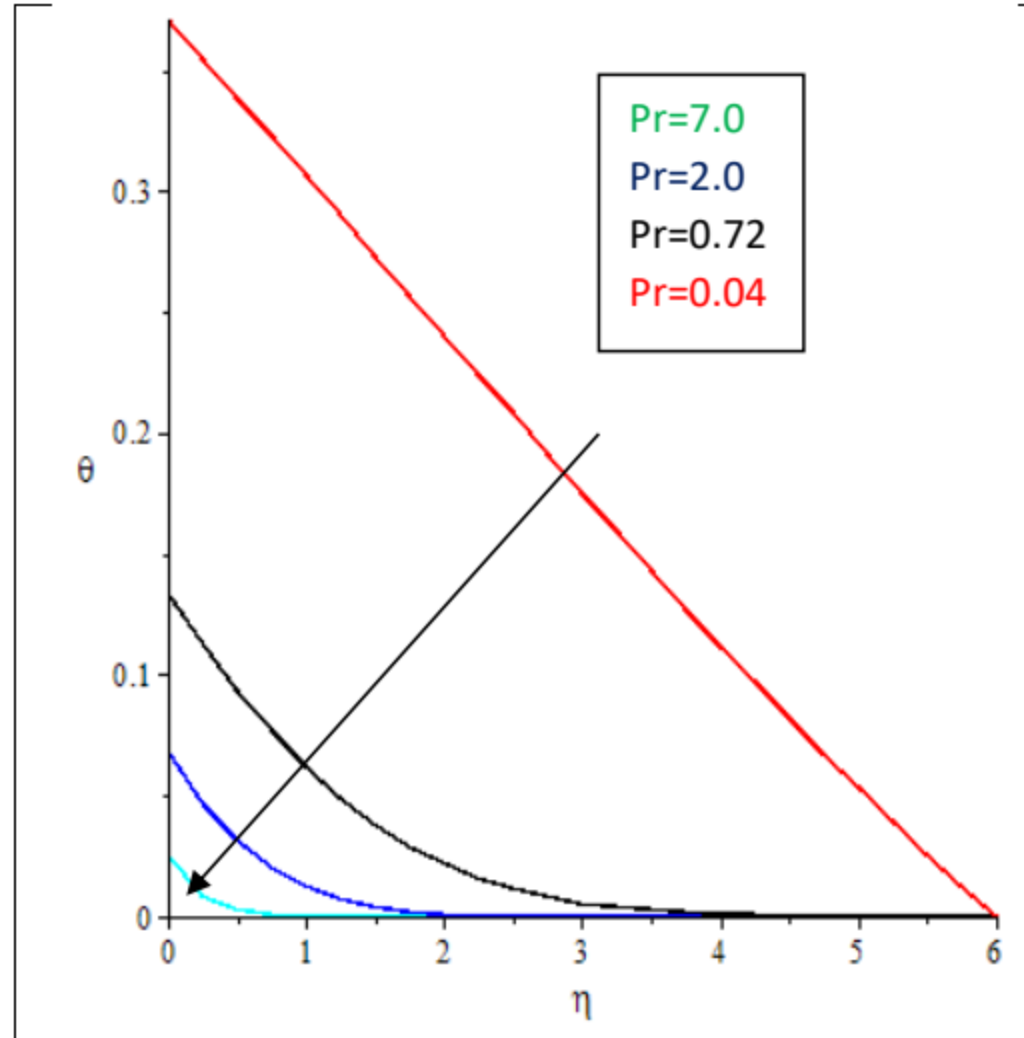


Figure 4.9: Effect of Prandtl Number Variation on $\theta(\eta)$

Figure 4.9 depict the resultant effect of Prandtl Number Variation on temperature profile $\theta(\eta)$, which shows that as Prandtl Number increases, the temperature of the fluid decreases rapidly. Hence an increase in Prandtl Number decreases the temperature profile of the fluid. This is because Prandtl number is a dimensionless number that represents the ratio of momentum diffusivity to thermal diffusivity in a fluid. When the Prandtl number is increased, it means that the thermal diffusivity of the fluid is relatively smaller compared to its momentum diffusivity. In a vertical fluid flow, an increase in the Prandtl number means that the fluid is less effective at conducting heat compared to its ability to transfer momentum. This results in a decrease in the rate of heat transfer within the fluid, leading to a flatter temperature profile.

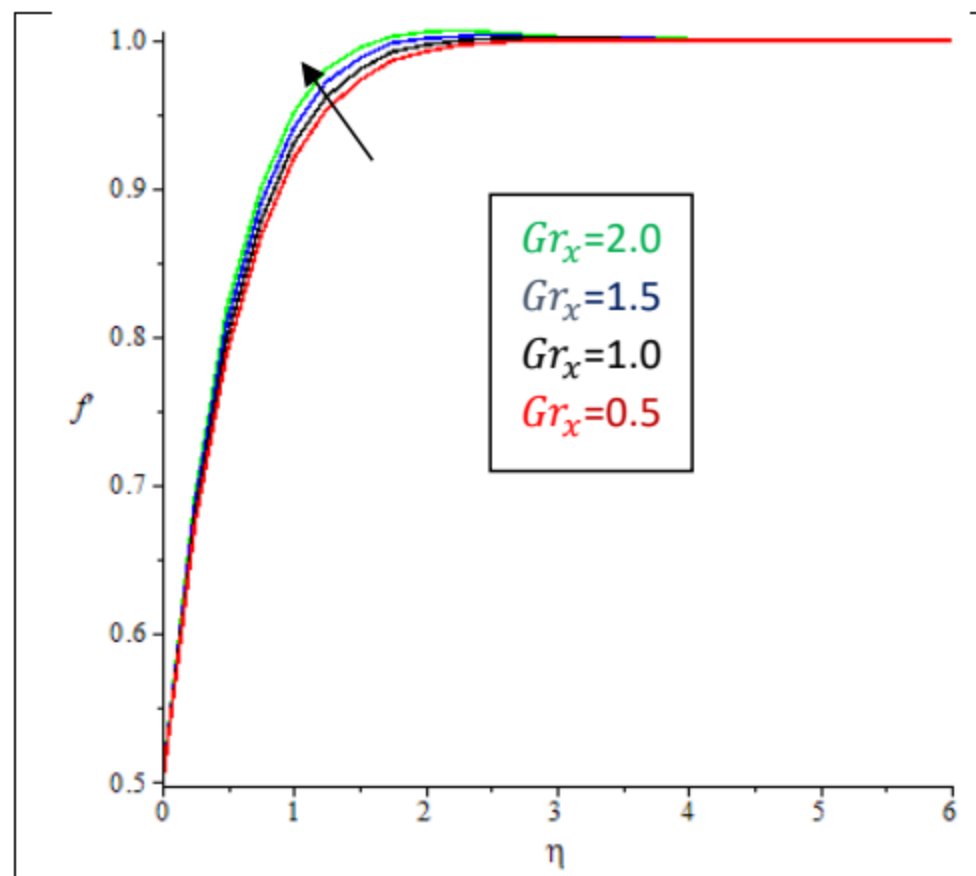


Figure 4.10: Effect of Convective Gr_x parameter on $f'(\eta)$

The consequences of Gr_x parameter on velocity profile is shown in figure 4.10. It is evident from the figure that Gr_x parameter has an increasing effect on velocity profile. This is because Gr_x strengthens the buoyancy force, and in turn enhances the fluid velocity.

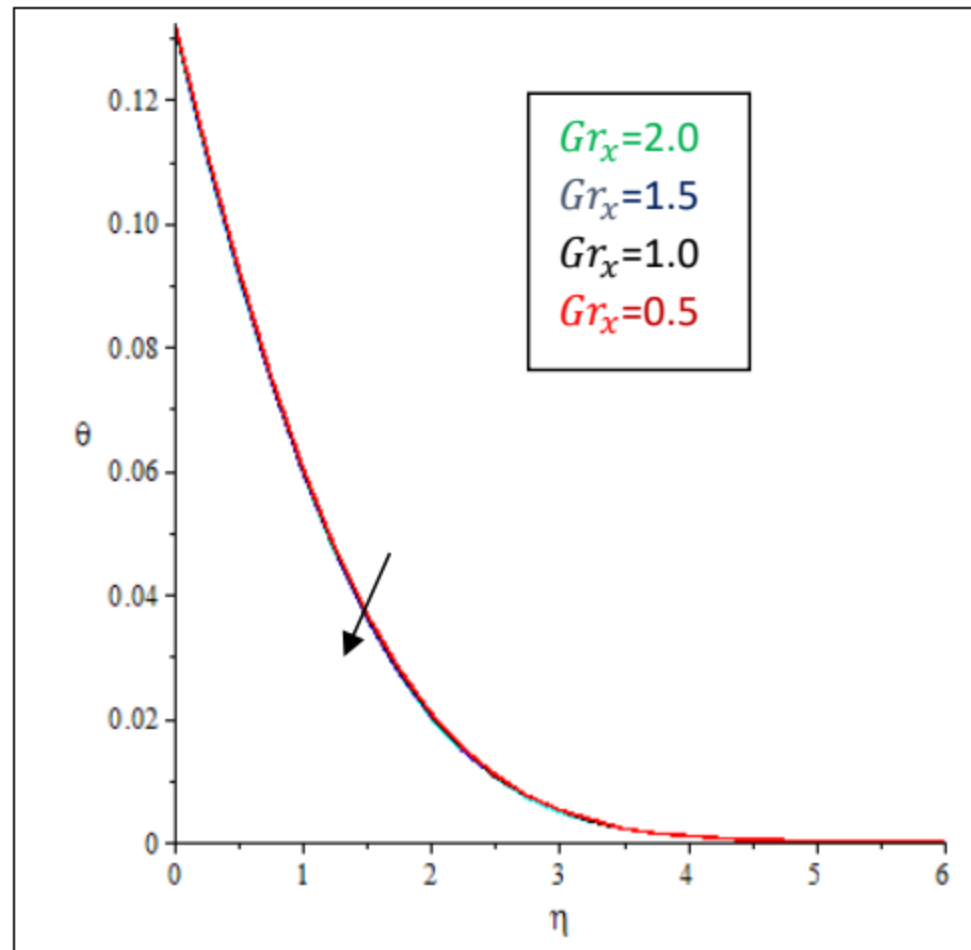


Figure 4.11: Effect of Convective Gr_x parameter on $\theta(\eta)$ for model 1

Figure 4.11 depict the resultant effect of Convective Gr_x parameter on temperature profile $\theta(\eta)$, which shows that as Convective Gr_x increases from 0.0 - 2.0, the temperature tend to decrease, although the difference in decrease from one point of Convective Gr_x parameter ranging from 0.0 - 2.0 is relatively low.

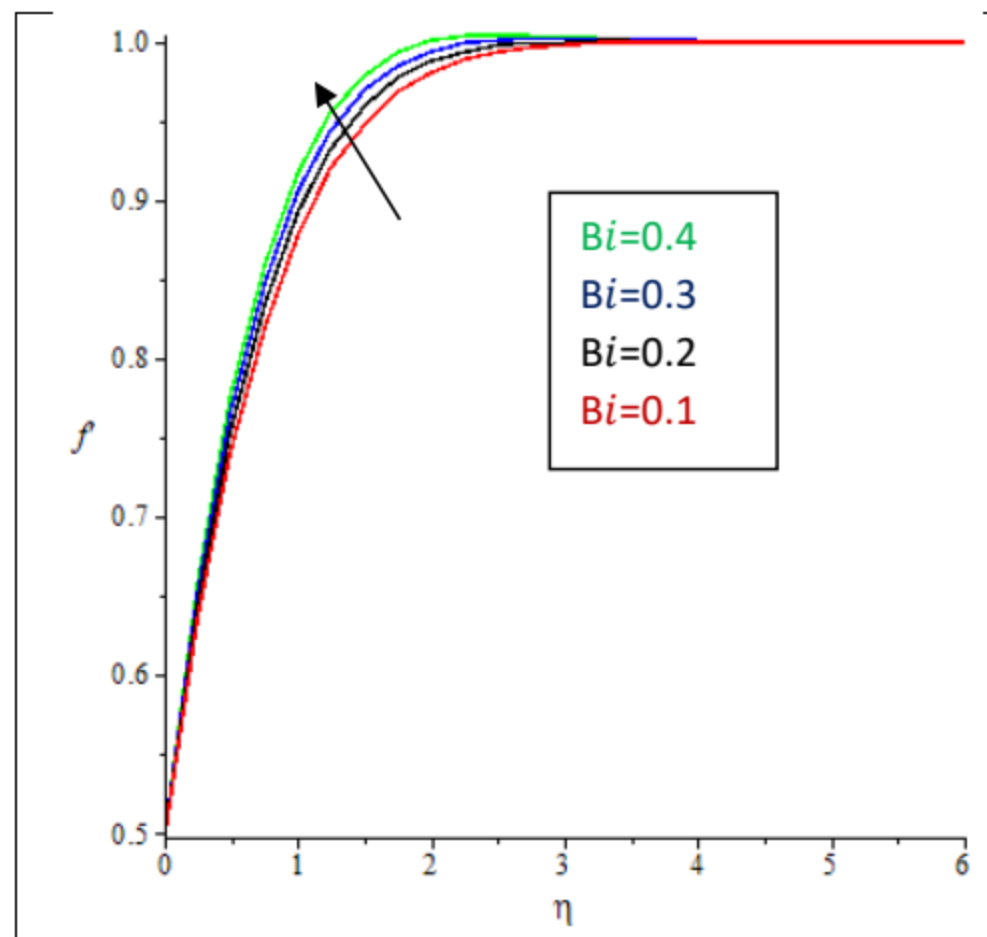


Figure 4.12: Effect of Bi number Variations on $f'(\eta)$

Figure 4.12 illustrates how varying the Bi number affects the velocity profile $f'(\eta)$. The graph demonstrates that an increase in the Bi number results in a corresponding increase in velocity profile of the system.

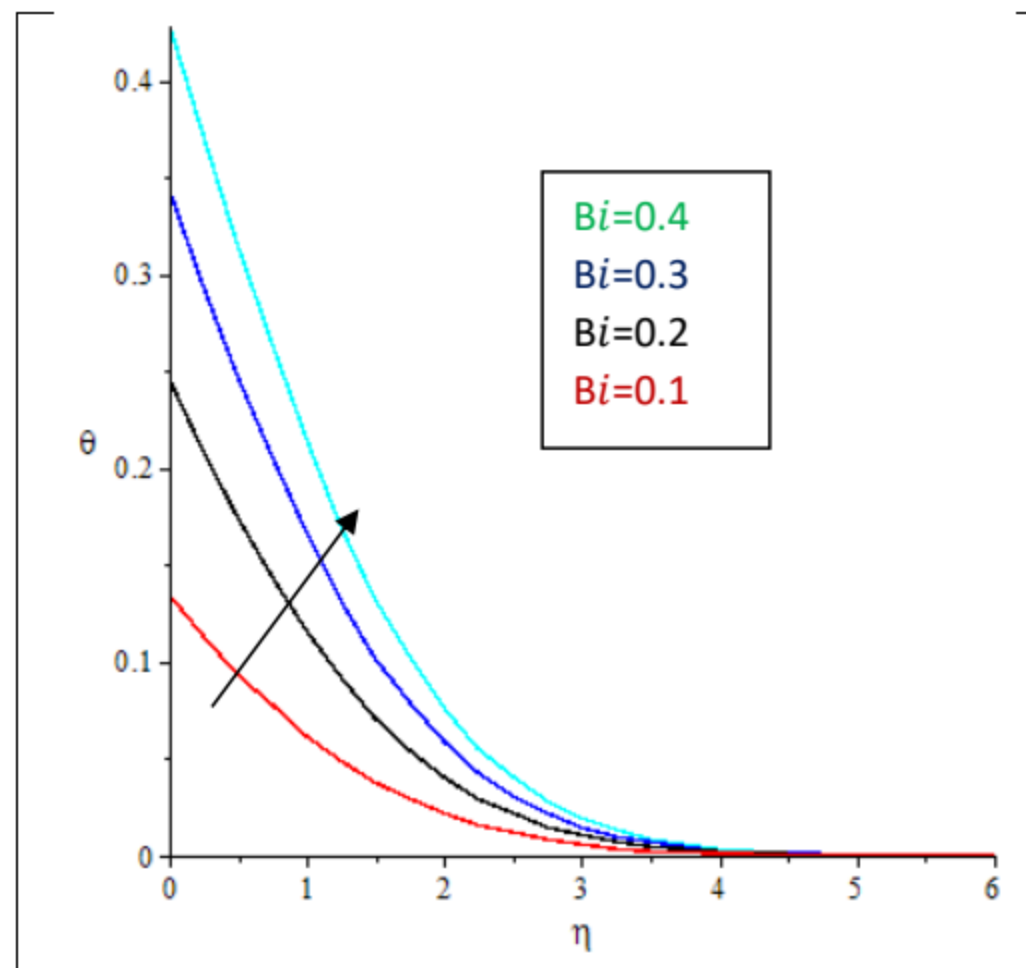


Figure 4.13: Effect of Bi variations on $\theta(\eta)$ for model 1

Figure 4.13 shows the effect of Bi number variation on temperature profile, it depicted that as the Bi number increases the temperature profile increase. This is because the Bi number is a dimensionless number used in heat transfer calculations to determine the relative importance of heat conduction within an object compared to heat convection at the object's surface. A higher Bi number indicates that convection heat transfer is more significant than conduction heat transfer. When the Bi number increases, it means that the rate of heat transfer through convection at the object's surface is higher relative to the rate of heat transfer through conduction within the object. In a fluid flow in a vertical direction, an increase in the Bi number means that there is more efficient convective heat transfer occurring at the surface of the fluid. This increased convective heat transfer leads to a more efficient exchange of heat between the fluid and its surroundings, resulting in a higher temperature profile within the fluid.

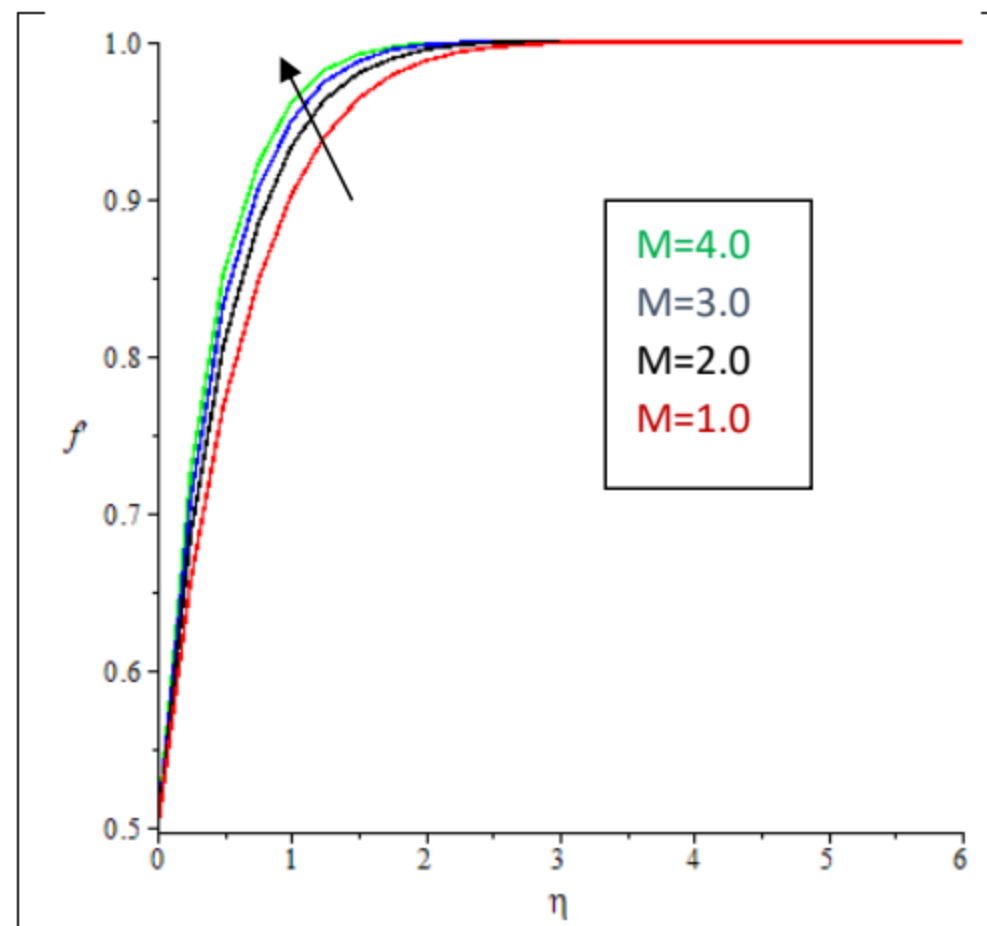


Figure 4.14: Effect of Magnetic Parameter Variations on $f'(\eta)$

Figure 4.14 show the effect of magnetic parameter variation on velocity profile, as illustrated from the figure, an increase in magnetic parameter leads to a corresponding increase in the velocity profile of the system. This is because an increase in the magnetic parameter can increase the velocity profile of the fluid due to the phenomenon known as magnetohydrodynamics (MHD). MHD is the study of the motion of electrically conducting fluids in the presence of a magnetic field. When a magnetic field is applied to a conducting fluid, it can exert a force on the fluid particles, causing them to move in a certain direction. This can lead to changes in the flow behavior of the fluid, resulting in an increase in velocity.

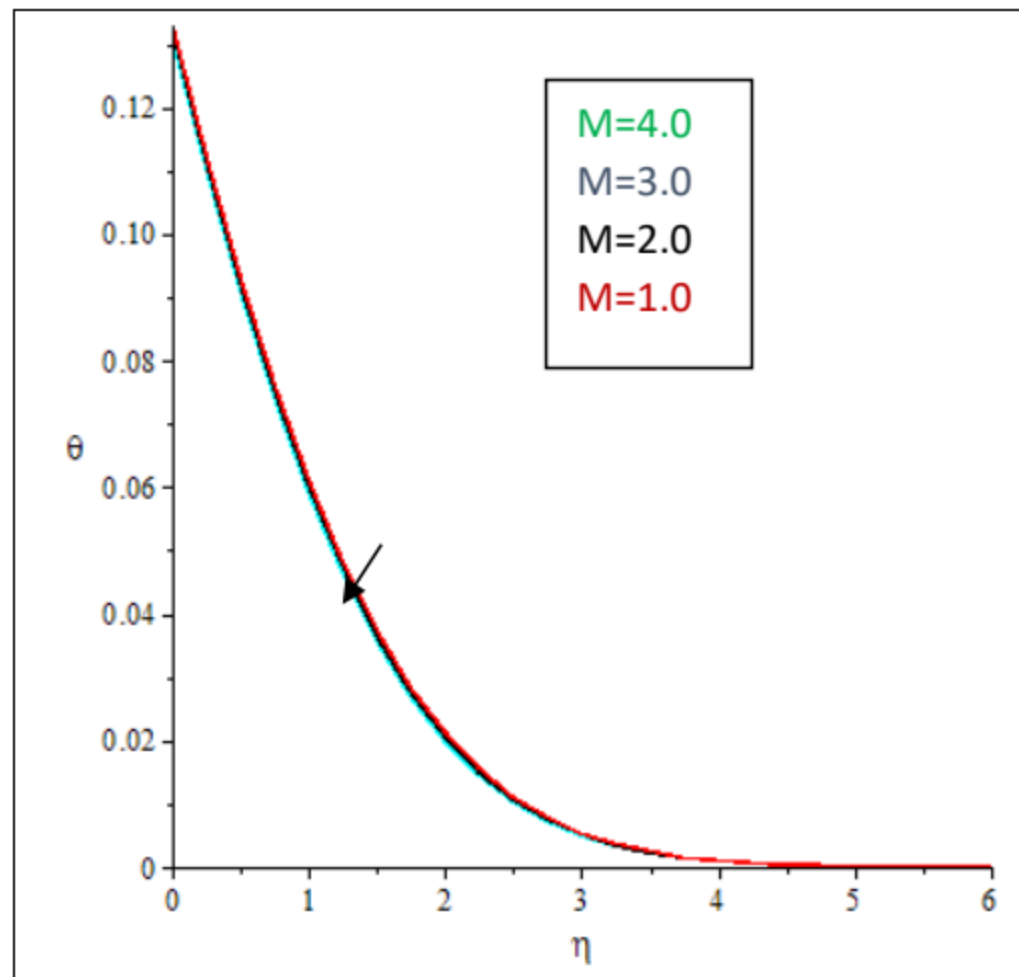


Figure 4.15: Effect of Magnetic Parameter Variations on $\theta(\eta)$

A resultant effect of magnetic parameter on temperature profile is depicted in figure 4.15. As shown from the figure, the magnetic parameter has a decreasing effect on the temperature profile. As the magnetic parameter increase the temperature decrease relatively low. Hence the magnetic parameter has little effect on the temperature profile of the system.

5. Conclusion

The investigation of mixed convection effect on MHD flow near a vertical porous plate under the influence of magnetic effect and velocity ratio with convective boundary conditions and nonlinear thermal radiation revealed the intricacies of fluid motion and heat transfer in such systems. The findings highlighted the significance of considering these effects in the analysis of MHD flows, as they significantly influenced the velocity and temperature profiles. The major conclusions of this study are:

- The presence of mixed convection parameter enhances the velocity profile in the system, leading to a reduction in both the temperature and concentration profiles. Additionally, the boundary layer thickness increases for all profiles.
- The magnetic parameter shrinks the velocity profile and thickens the boundary layer whereas the temperature distribution rises with the boundary layer thinning thinner due to the influence of the Lorentz force.
- As the velocity ratio increases, the velocity profile is enhanced, resulting in a thicker boundary layer, whereas the temperature profile experiences a decrease.

- The Boit number results in improved velocity and temperature profiles, causing an increase in thickness for both boundary layers.

Finally the study emphasized the importance of considering these effects, as they had a substantial impact on the heat and mass transfer rates near the porous plate.

REFERENCES

- Aaiza, G., Ilyas, K., & Sharidan, S.(2015). Energy Transfer in Mixed Convection MHD flow of Nanofluid Containing Different Shapes of Nanoparticles in a Channel Filled with Saturated Porous Medium. *Journal of Nano Research Letters*. 10(1), 490-504
- Alamri S., Ambreen A., Mariam A., & Ellahi R. (2019). Effect of Mass Transfer on MHD Second Grade Fluids Towards Stretching Cylinder. *Journal of Physics Letters A*. 383(2-3), 276-281
- Alfvén, H. (1942). Existence of Electromagnetic-Hydrodynamic Waves. *Journal of Nature*. 150(3805),405-406
- Ali Agha H., Bouaziz. M.N, Hanini S.,(2014). Free Convection Boundary Layer Flow from a Vertical Flat Plate Embedded in a Darcy Porous Medium Filled with Nanofluid : Effect of Magnetic Field and Thermal Radiaton. *Arab Journal of Science Engineering*.39(11), 8331-8340.
- Davood D., & Sayyid H.K. (2015). Natural,Mixed and Force Convection in Nanofluid. *JournalofApplication of Nonlinear Systems in Nanomechanics and Nanofluid*.9(6)205-269
- Hemalatha K. & Prasad S.R. (2014). Melting with Viscous Dissipation on MHD Radiative flow from a Vertical Plate Embedded in Non-Darcy Porous Medium. *Journal of Applied Fluid Mechanics* 8(4), 747-752.
- Jha B.K., Isah B.Y., & Uwanta I.L.,(2018). Combined Effect of Suction/Injection on MHD Free Convection Flow in a Vertical Channel with Thermal Radiation. *Ain Shams Engineering Journal*. 9(4), 1069-1088.
- Jha K. B., & Mohammed U. (2014). Mixed Convection Effect on Melting From a Vertical Plate Embedded in a Saturated Porous Media. *Journal of Heat Transfer- Asian Research*. 43(7)667-676
- Jha K. B., & Samaila G. (2021a). Numerical Solution for Natural Convection flow near a Vertical Porous Plate Having Convective Boundary Condition with Nonlinear Thermal Radiation. *Journal of Heat Transfer* 51(9) 45-60
- Jha, B. K.,Mohammed, U. & Abiodun, O. (2013). Dufour and Soret Effects on Melting from a Vertical Plate Embedded in Saturated Porous Media. *Journal of Applied Mathematics*. 2013(1), 9-20
- Jha, K., and Muhammad, S. (2019). Chemical Reaction and Dufour Effect on Nonlinear Free Convection Heat and Mass Transfer flow near a Vertical Moving Porous Plate. *Journal of Heat Transfer-Asian Research*. 49(1), 1-16.
- Jha, K.and Samaila, G. (2020).Similarity Solution for Natural Convection Flow near a Vertical Plate with Thermal Radiation. *Journal of Microgravity Science and Technology*. 32(1), 1031-1038
- Jha, K.B, & Samaila, G. (2021b). Impact of Nonlinear Thermal Radiation on Nonlinear Mixed Convection Flow near a Vertical Porous Plate with Convective Boundary Condition. *Journal of Process Mechanical Engineering*. 236(2)689-703

- Jha, K.B. & Samaila, G. (2022). Thermal Radiation Effect on Boundary Layer over a Flat Plate having Convective Surface Boundary Condition. *Springer Nature Journal of Applied Science*. 2(1), 381-398.
- Reddy, S. & Ali, J. (2016). Soret and Dufour Effect on MHD Heat and Mass Transfer Flow of a Micropolar Fluid with Thermophoresis Particle Deposition. *Journal of Naval Architecture and Marine Engineering*. 13(1) 239-270.
- Saman R., Javad A., & Mahla M. (2017). Application of Magnetohydrodynamics in Biological Systems – A Review on the Numerical Studies. *Journal of Magnetism and Magnetic Materials*, 439(1), 358-372.
- Sharma P., Sharad S., Yadav R., & Anatoly N. (2018). MHD Mixed Convective Stagnation Point Flow along a Vertical Stretching Sheet with Heat Source/Sink. *International Journal of Heat and Mass Transfer*. 117(1) 780-786.
- Surbhi S., Amit D., Amit P., Jyoti A., Qasem A., (2023). Analysis for MHD Micro Polar Fluid over a Melting Stretching Surface with Slip Effect. *Research Gate Journal* 13(1), 562-578.
- Venkata, R., Anantha, K., & Sandeep, N. (2021). Impact of Soret and Dufour on MHD Casson Fluid Flow Pass a Stretching Surface with Convective-Diffusive Conditions. *Journal of Thermal Analysis and Calorimetry*. 147(1), 2653-2663.